Latitudinal gradient in aerosol properties over the Indian and Southern Oceans during the austral summer

S. Suresh Babu[1], K. Krishna Moorthy[1] and S. K. Satheesh[2],*

[1]Space Physics Laboratory, Vikram Sarabhai Space Centre, Thiruvananthapuram 695 022, India
[2]Centre for Atmospheric and Oceanic Sciences, Indian Institute of Science, Bangalore 560 012, India

Extensive measurements of columnar aerosol optical depth (AOD), composite (M_T) and black carbon aerosol mass (M_B) concentrations were made over the tropical Indian and Southern Oceans as a part of the Pilot Expedition to the Southern Ocean during the boreal winter. The AOD, M_T and M_B show large latitudinal gradient towards south up to ITCZ. Beyond ITCZ, up to 56°S, AOD and M_B show very low and steady values. However M_T shows large variations in the Southern Ocean due to the enhanced production of sea salt aerosols associated with high sea surface winds. The short wave aerosol radiative forcing at the surface over north of equator is in the range −10 to −23 W m^{-2}, whereas that over the Southern Ocean was in the range −4 to −5 W m^{-2}. The corresponding atmospheric forcing was in the range of 6–13 W m^{-2} and 0.8–1.4 W m^{-2}. This large north–south change in the aerosol radiative forcing has important implications to the meridional circulation and hence to climate.

Keywords: Aerosol, black carbon, optical depth, Southern Ocean.

Introduction

STUDIES of atmospheric aerosols over oceanic regions have significance from the perspective of understanding marine aerosols, estimating their direct and indirect roles in regional and global radiative forcing, and in delineating the effects of long-range transport of continental aerosols on marine environments. Several field campaigns during the last decade have specifically focused on this over distinct regions. Examples are ACE I and II[1,2], TARFOX[3], SCAR-A[4], INDOEX[5] and the ACE-Asia[6]. Earlier studies revealed a decrease in the aerosol concentration with increase in distance from the mainland[7–10]. However, most of these studies were restricted to 20°S and limited to either columnar aerosol optical depth (AOD) or composite aerosol. None of them had observations of absorbing aerosols such as black carbon and observations south of 20°S.

In view of the above, a thematic experiment to characterize aerosols was planned onboard the *ORV Sagar Kanya* during January–March 2004, during its first expedition to the Southern Ocean (SO). Here we present data on columnar AOD along with total and black carbon aerosol mass concentrations over the Indian Ocean and SO. The estimates of aerosol radiative forcing over different latitude sectors are also presented.

Experimental setup and data collection

The three-month long expedition was conducted in three phases; (i) *the initial phase* (SK199) from 1 to 19 January 2004 from Kochi to Mauritius (MRU) surveyed the Arabian Sea and the tropical Indian Ocean, (ii) *the main phase* (SK200) from 24 January to 4 March focused on the SO and (iii) *the final phase* (SK201) from 11 to 30 March pertained almost the same region as the initial phase, but after about two months. The cruise tracks are shown in Figure 1. The aerosol measurements comprised of ambient mass concentrations of composite and BC aerosols, made respectively using a single stage high volume sampler (HVS model GHV2000P1 of Thermo-Anderson) and a dual beam Aethalometer (AE-21 of Magee Scientific, USA), and columnar spectral optical depths made using a Microtops sunphotometer.

The Aethalometer was kept inside the ship's cabin and ambient air was taken through an inlet pipe from the bow side (sampling into the wind) of the ship. The air intake was from a height of about 12 m from the sea level. The flow rate was kept at 5 litres per minute (lpm) during the first phase and increased to the maximum value (6.8 lpm) permissible for the instrument in SO. The time base also was increased from 5 min in the tropical ocean to 60 min in SO in view of the extremely low concentration encountered there. Following the error budget, discussed earlier[11,12], the maximum uncertainty in the measured BC was 15% in SO, and was 10% and 8% in the tropical Indian Ocean and SO respectively.

The high volume sampler, for estimating the mass concentration of composite aerosol, was operated from the front deck of the ship and sampling was done facing the wind flow. Quartz fibre discs of 4-inch diameter were

used as the collection substrates. The mean flow rate was $0.6 \, m^3 \, min^{-1}$ and the calibration was ensured before and after the campaign period using a calibration setup. The quartz fibre substrates were preheated in an oven to 100°C and then desiccated for 24 h. These substrates were then tare weighed using a microbalance (Model AT 120, Metler) with a precision of $\pm 2 \, \mu g$ and sealed in separate numbered self-locking envelopes. Tare weighed substrate from the envelope is mounted on the impactor and aerosols samples were collected by operating it for 3–10 h. After sampling, substrates were sealed in the respective envelopes. In the laboratory these were on for 24 h and then were weighed using the same balance in the same room conditions. The difference between the final and tare weights gave the aerosol mass loading. Knowing the volume of air sampled (the flow rate times sampling duration), the mass concentration was estimated.

Spectral AOD measurements were made onboard using a hand-held Microtops (MTOPS) sunphotometer at four wavelengths 380, 500, 675 and 870 nm primarily due to the ease of handling and also because of its capability to yield AOD from each measurement, which is of great advantage on cruise platforms. Adequate care was taken in collecting this data onboard the ship following the necessary precautions and considerations[13,14].

Results and discussion

Spectral aerosol optical depths

The AOD at 500 nm measured using MTOPS, averaged over a day, are plotted against the corresponding latitude in Figure 2. The AOD values during SK199 (January),
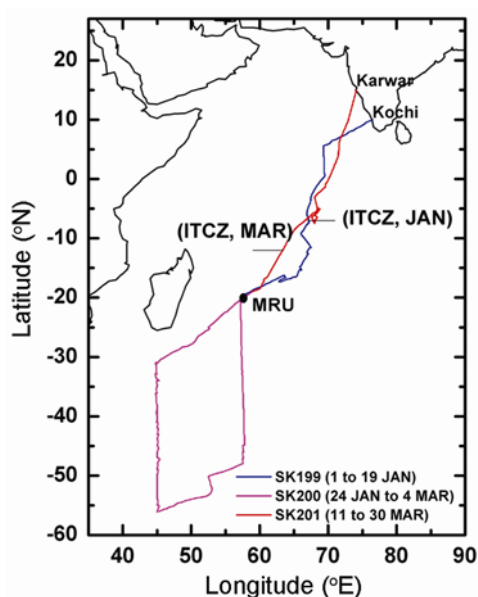
SK200 (February) and SK201 (March) are represented by solid triangle, circle and star, respectively. Between 10°N and 20°S, the cruise tracks in SK199 (January) and SK201 (March) are very close and hence the longitudinal differences in AOD can be neglected. However there is a time gap of ∼ 2 months between SK199 and SK201, hence data obtained from each cruise are treated separately. AOD shows significant latitudinal gradient to the north of 20°S, both during January and March. The prevailing winds over the study area during the three cruise periods are shown in Figure 3. Examination of these winds and outgoing long wave radiation (OLR) from the National Centre for Environmental Prediction (NCEP) data shows that in January the mean position of ITCZ (region of convergence of northerly and southerly circulations) was around 7°S in the longitude sector 60°–75°E (where the cruise track lies) whereas during March the ITCZ moved further south and located around 12°S in the above longitude sector. Interestingly, the latitude gradient in AOD persisted up to ITCZ; thereafter the AOD values in both periods are comparable to the SO values. To the north of the equator, the latitudinaly averaged (10°N to 0°) value of columnar AOD during January was 0.32 ± 0.01, which slightly increased to 0.38 ± 0.07 during March. The corresponding values to the south of the equator (0° to 10°S) are 0.12 ± 0.02 and 0.17 ± 0.04. In SO (20°S to 56°S) AOD values varied between 0.10 and 0.15 (with a mean value of 0.11 ± 0.003) without any latitude dependence.

Spectral variation of AOD provides information on its size characteristics and can be expressed by using the Angstrom power law given by,

$$\tau_{a\lambda} = \beta \lambda^{-\alpha}, \tag{1}$$

where α is the wavelength exponent indicating the size distribution, β the turbidity parameter indicating the aerosol

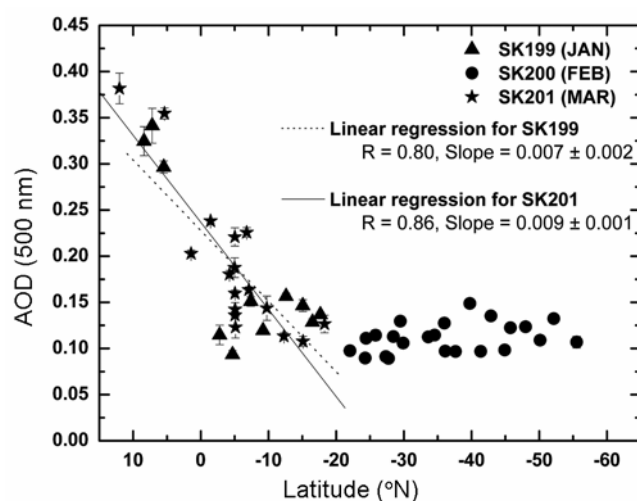**Figure 1.** Cruise tracks for SK199, SK200 and SK201.

Figure 2. Latitudinal variation in AOD over the tropical and the Southern Oceans.
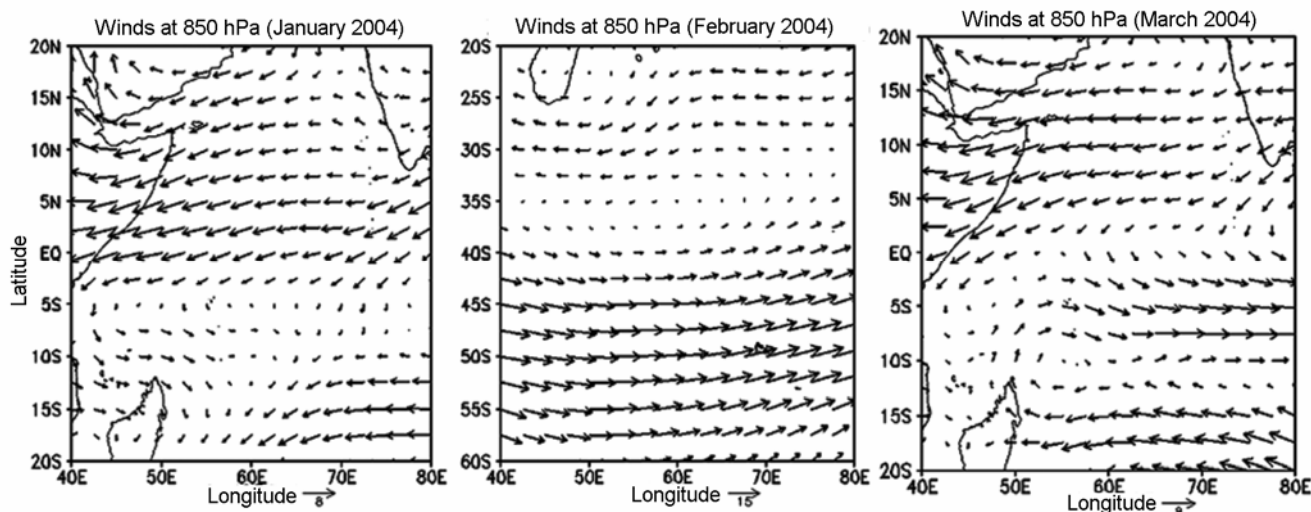
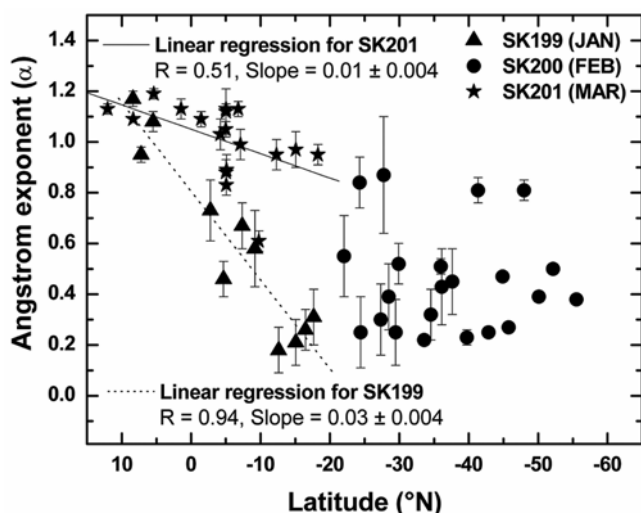**Figure 3.** Wind fields for January, February and March 2004.

Figure 4. Latitudinal variation in α over the tropical and the Southern Oceans.

Figure 5. Spatial variation of BC mass concentration.

loading and λ the wavelength in $\mu m^{7,9}$. Lower values of α indicate relatively larger abundance of super micron aerosols. Using a least squares fit between τ_a and λ on a log–log scale α and β were evaluated. The latitudinal variations of α values are shown in Figure 4. In the tropical oceanic regions, α values show steep gradient with latitude during January. During March the gradient in α becomes weaker. The latitude gradient in α is found to be 0.03 during January, which reduces to 0.01 during March. This may be due to the change in the direction of winds to the south of equator during March (Figure 3), where the wind changes its direction from northeasterlies to westerlies bringing aerosols of continental origin (contains smaller particles) from the adjacent African continent. These aerosols may be responsible for the weaker gradients in α during March. Over the SO, the α values
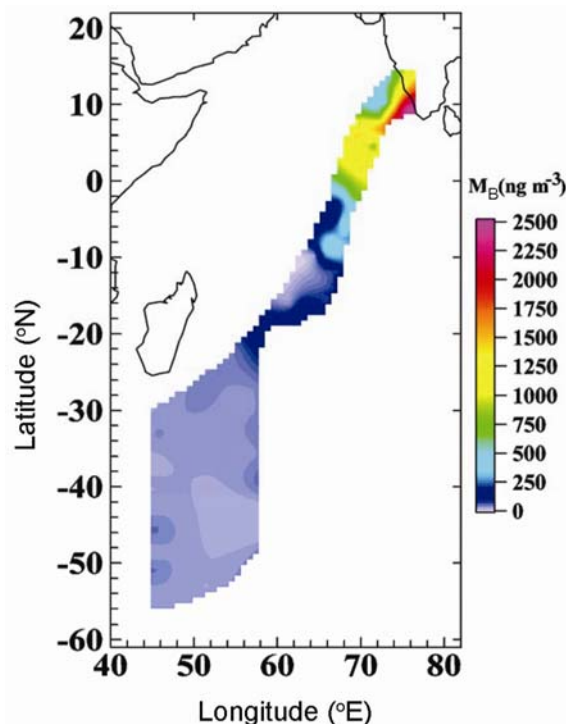
fell in a wide range of values between 0.2 and 0.8 (with a mean value of 0.45 ± 0.04) over different latitudes without any latitude dependence.

Aerosol black carbon

The spatial variation of BC mass concentration (M_B) measured using Aethalometer is shown in Figure 5, considering the entire data as samples drawn from a popula-

tion. It clearly shows: (i) high concentrations of BC (> 1000 ng m^{-3}) over the oceanic regions north of the equator; (ii) a rapid decrease in the concentrations towards south, reaching values below 200 ng m^{-3} at Mauritius; (iii) extremely low concentrations ($\leq \sim 50$ ng m^{-3}) in SO; (iv) the decrease in M_B with latitude is conspicuous up to the ITCZ; beyond ITCZ, values remained more or less the same.

To parameterize the latitudinal variation of M_B, the data is grouped into latitudinal bins of 1° width and averaged. In this case also, in view of the ~ 3 months time span over which the measurements were made, the data in each phase were considered separately. The results shown in the bottom panel of Figure 6 reveal that: (i) M_B is very low and shows insignificant latitude variation to the south of $\sim 10°$S, with a mean value of 30 ± 10 ng m^{-3} for SO; (ii) north of 10°S, the concentration increases rapidly. The rate of increase is higher during January than in March.

The latitudinal variation of M_B due north of MRU was parameterized using an exponential growth function of the form

$$M_B(\Lambda) = A \exp(\Lambda / \Lambda_s), \qquad (2)$$

where $M_B(\Lambda)$ is the BC concentration at a latitude Λ, A the amplitude of the growth (numerically equal to the concentration at the equator) and Λ_s is the scaling distance (in degrees of latitude) for which the M_B grows e-fold. The scaling distance during January is 7.5°, which increases to 9.25° during March showing a weaker latitudinal gradient during the latter period. The amplitude also decreases from ~ 640 ng m^{-3} in winter to ~ 290 ng m^{-3} in inter-monsoon.

Composite aerosol

Not only BC, but the composite aerosol also showed latitudinal variations. The latitudinal variation of composite aerosol mass concentration (M_T) is shown in the top panel of Figure 6. Similar to AOD and M_B, M_T also decreases with latitude up to ITCZ. This latitudinal variation also can be parameterized using eq. (2) by replacing M_B with M_T. The scaling distance in this case is found to be 9.48° with amplitude of 1640 ng m^{-3}. The scaling distance obtained in the case of M_T is comparable to that of M_B during the same period. However in SO, the M_T values are highly variable, with high values being associated with gusty conditions encountered during the cruise. Examination of the wind speed dependency of the M_T values showed that an exponential increase with an index of 0.13, indicating the role of increased sea-spray production by the high winds.

Using the collocated measurements of BC and composite aerosols, the mass mixing ratio of BC (F_{BC}) was estimated, and its latitudinal variation is examined in Figure 7, where the points are experimentally determined mixing ratio and the dotted line is the best fit curve. It is interesting to note that F_{BC} shows a sharp peak at $\sim 1°$N, with an amplitude of $\sim 3\%$, and falls off on either side to low values. As F_{BC}, rather than M_B, is important in radiative forcing, this observation indicates increased forcing at locations far away from potential sources of BC. Interestingly in SO, F_{BC} is found to be very low, $\sim 0.2\%$.

Aerosol radiative forcing

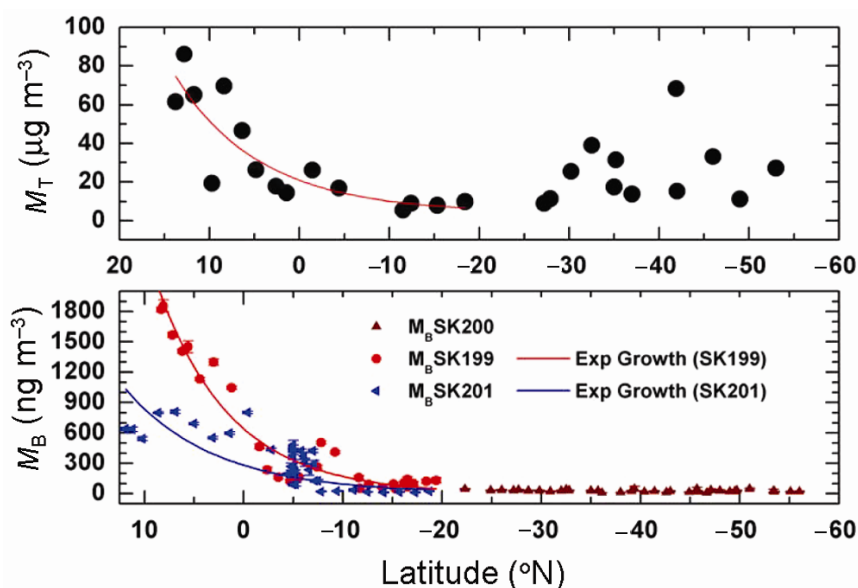The above characteristics of aerosols were used to estimate the direct short wave radiative forcing over the

Figure 6. Latitudinal variation in M_T (top panel) and M_B (bottom panel) over the tropical and Southern Oceans.
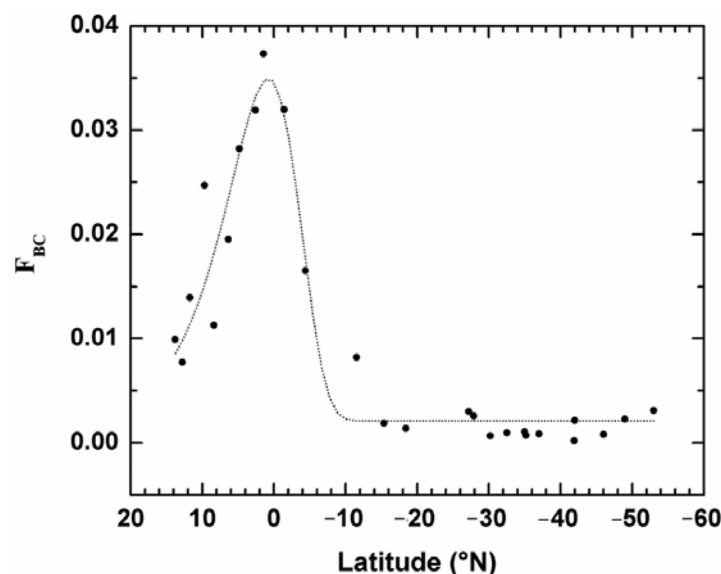
Figure 7. Latitudinal variation in F_{BC} over the tropical and the Southern Oceans where the points represent the F_{BC} values at each latitude and the continuous line through the points represents the best fit.

Table 1. Aerosol forcing estimated for various latitude sectors

Latitude sector	ω (500 nm)	TOA forcing (W m^{-2})	Surface forcing (W m^{-2})	Atmospheric forcing (W m^{-2})
10°N to 0°	0.91	−10.14 ± 4.9	−22.9 ± 11.8	12.8 ± 6.9
0° to 10°S	0.92	−5.0 ± 0.81	−11.4 ± 2.0	6.4 ± 1.2
10°S to 20°S	0.98	−3.8 ± 0.35	−5.2 ± 0.6	1.4 ± 0.21
Southern Ocean	0.99	−3.9 ± 0.7	−4.7 ± 0.7	0.8 ± 0.05

different sectors of the tropical Indian Ocean and SO. For this we used the available observations as anchoring points in appropriate marine aerosol models[15], which is fine-tuned to match the optical properties with the measurements. Based on our observations of AOD, α, M_T, M_B and F_{BC} we have divided the study region into four latitudinal sectors, viz. 10°N to equator, equator to 10°S, 10°–20°S and SO (20°–56°S) and adopted the maritime polluted model for the northern tropical ocean, southern tropical ocean and the maritime background model in SO and used the F_{BC} values, spectral AODs and α values as anchoring points. The relative abundance of non-measured components was varied such that the spectral AODs estimated for the composite aerosol model in each sector agreed with the corresponding observed mean values of spectral AODs for each sector in general. Using these aerosol models, the single scattering albedo (ω) and phase function were estimated for each sector as a function of wavelength. The value of ω estimated for each sector at 500 nm is given in Table 1.

To compute the aerosol radiative forcing we have used the Santa Barbara DISORT Atmospheric Radiative Transfer (SBDART)[16]. The experimental values of spectralAOD and α along with the estimated values of ω and phase function were incorporated into SBDART to estimate the diurnally averaged clear sky short wave radiative forcing. The short wave radiative forcing thus estimated at TOA, surface and in the atmosphere for each sector is given in Table 1. The short-wave aerosol radiative forcing at TOA in the latitude sector 10°N to 0°N was in the range of −15.3 to −5.5 W m^{-2} and corresponding forcing at the surface was in the range −35.4 to −11.9 W m^{-2}. Beyond equator, up to 10°S the magnitude of forcing reduces drastically maintaining the surface to TOA forcing ratio almost same. These estimates are made for the latitude sectors north of ITCZ where the influences of anthropogenic aerosols from adjacent continental areas are significant. South of ITCZ, the magnitude of forcing is low and more or less the same without any latitude dependence.

Conclusions

Collocated measurements of columnar AOD, composite aerosol mass concentration and black carbon mass concentration were made during the trans-continental cruise experiment during January–March 2004 over the Indian

Ocean and the SO. All the aerosol parameters show latitudinal gradient towards south up to ITCZ. The latitudinal gradient is found to be steeper during January and weaker in March. The mean value of columnar AOD over the north of the equator was in the range 0.32–0.38, which reduces to ~0.11 over the SO. Similarly the BC mass concentration in the range 2 (in January) to 0.7 $\mu g\,m^{-3}$ (in March), north of equator reduces to <50 ng m^{-3} over SO. Both AOD and M_B show rather steady values over SO. Even though M_T shows latitudinal variations similar to that of AOD and M_B to the north of ITCZ, it shows large variations in SO due to the enhanced production of sea salt aerosols associated with the high sea surface winds. The short wave aerosol radiative forcing at the surface over north of the equator is in the range – 10 to – 30 W m^{-2}, whereas that over SO it was in the range – 4 to – 5 W m^{-2}. The corresponding atmospheric forcing was in the range of 6 to 13 W m^{-2} and 0.8 to 1.0 W m^{-2}.

1. Bates, T. S., Huebert, B. J., Gras, J. L., Griffiths, F. B. and Durkee, P. A., International Global Atmospheric Chemistry (IGAC) project's first aerosol experiment (ACE 1): overview. *J. Geophys. Res.*, 1998, **103**, 16297–16318.

2. Raes, F., Bates, T., McGovern, F. M. and van Liederkerte, M., The second Aerosol Characterization Experiment (ACE-2): general overview and main results. *Tellus*, 2000, **52B**, 111–126.

3. Russell, P. B., Hobbs, P. V. and Stowe, L. L., Aerosol properties and radiative effects in the United States East Coast haze plume: an overview of Tropospheric Aerosol Radiative Forcing Observational Experiment (TARFOX). *J. Geophys. Res.*, 1999, **104**, 2213–2222.

4. Kaufman, Y. J. and Holben, B. N., Hemispherical backscattering by biomass burning and sulfate particles derived from sky measurements. *J. Geophys. Res.*, 1996, **101**, 19433–19445.

5. Ramanathan, V. *et al.*, Indian Ocean Experiment: an integrated analysis of the climate forcing and effects of the great Indo-Asian haze. *J. Geophys. Res.*, 2001, **106**, 28371–28398.

6. Huebert, B. J. *et al.*, An overview of ACE-Asia: Strategies for quantifying the relationships between Asian aerosols and their climatic impacts. *J. Geophys. Res.*, 2003, **108**, 10.1029/2003JD003550.

7. Moorthy, K. K., Satheesh, S. K. and Murthy, B. V. K., Investigations of marine aerosols over the tropical Indian Ocean. *J. Geophys. Res.*, 1997, **102**, 18827–18842.

8. Jayaraman, A., Lubin, D., Ramachandran, S., Ramanathan, V., Woodbridge, E., Collins, W. and Zalpuri, K. S., Direct observations of aerosol radiative forcing over the tropical Indian Ocean during the January–February 1996 pre-INDOEX cruise. *J. Geophys. Res.*, 1998, **103**, 13827–13836.

9. Satheesh, S. K., Moorthy, K. K. and Murthy, B. V. K., Spatial gradients in aerosol characteristics over the Arabian Sea and Indian Ocean. *J. Geophys. Res.*, 1998, **103**, 26183–26192.

10. Nair, P. R., Parameswaran, K., Kumar, S. V. S. and Rajan, R., Continental influence on the spatial distribution of particulate loading over the Indian Ocean during winter season. *J. Atmos. Sol. Terr. Phys.*, 2004, **66**, 27–38.

11. Babu, S. S. and Moorthy, K. K., Aerosol black carbon over a tropical coastal station in India. *Geophys. Res. Lett.*, 2002, **29**(23): art. no. 2098.

12. Babu, S. S., Moorthy, K. K. and Satheesh, S. K., Aerosol black carbon over Arabian Sea during inter monsoon and summer monsoon seasons. *Geophys. Res. Lett.*, 2004, **31**, L06104.

13. Ichoku, I. *et al.*, Analysis of the performance characteristics of the five-channel Microtops II sun photometer for measuring aerosol optical thickness and perceptible water vapour. *J. Geophys. Res.*, 2002, **107**, 10.1029/2001JD001302.

14. Porter, J. N., Miller, M., Pietras, C. and Motell, C., Ship based sun photometer measurements using Microtops sun photometer. *J. Atmos. Oceanic Technol.*, 2001, **18**, 765–774.

15. Hess, M., Koepke, P. and Schultz, I., Optical properties of aerosols and clouds: the software package OPAC. *Bull. Am. Meteorol. Soc.*, 1998, **79**, 831–844.

16. Ricchiazzi, P., Yang, S., Gautier, C. and Sowle, D., SBDART: a research and teaching tool for plane-parallel radiative transfer in the Earth's atmosphere. *Bull. Am. Meteorol. Soc.*, 1998, **79**, 2101–2114.